Int. J. Sci. R. Tech., 2026 3(7)
A Multidisciplinary peer-reviewed Journal
www.ijsrtjournal.com [ISSN: 2394-7063]

Original Article

In Silico Molecular Docking And ADMET Evaluation Of Coumarin Derivatives As Potential Therapeutic Lead Compounds

Vivekanand Ekanath Teli*, Rutuja Ashok Vyawahare, Bhumika Bhairu Mohite, Dipali Vijay Patil

Sant Gajanan Maharaj College of Pharmacy, Mahagaon, Maharashtra, India

ABSTRACT

Coumarin derivatives are important heterocyclic compounds exhibiting a wide range of pharmacological activities such as anticancer, anti-inflammatory, antioxidant, antimicrobial, and anticoagulant effects. In this study, computer-aided drug design (CADD) techniques were employed to evaluate the binding potential of selected coumarin derivatives toward a target protein. Molecular docking was carried out using AutoDock Vina to analyze ligand–protein interactions and binding affinities. The docking results revealed stable complexes supported by hydrogen bonding, hydrophobic interactions, and π–π stacking with key amino acid residues. Pharmacokinetic and drug-likeness properties were assessed using SwissADME, and all compounds complied with Lipinski's rule of five, indicating good oral bioavailability. ADMET predictions confirmed favorable absorption, low toxicity, and non-mutagenic behavior of the compounds. Among the tested molecules, warfarin showed the highest binding affinity when compared with the standard drug selegiline. Overall, the findings suggest that coumarin derivatives possess promising drug-like characteristics and may serve as potential lead molecules for further experimental and pharmacological studies. The software tools CHEMDRAW, PYMOL, AVOGADRO, BIOVIA DISCOVERY STUDIO, AUTO-DOCK VINA, SWISS ADME, PROTEIN DATA BANK, PUBCHEM, PROTEIN DATA BANK SUM.

Keywords: Coumarin derivatives; Molecular docking; In silico drug discovery; ADMET prediction; SwissADME; Drug-likeness; Virtual screening; Computational chemistry.

INTRODUCTION

Organic chemical compounds with a ring-like structure that contain one or more heteroatoms are referred to as heterocyclic compounds, or heterocycles. Both cyclic and acyclic heterocycles are possible. Although the overall structure of heterocycles is similar to that of cyclic organic compounds, which only contain one carbon atom, heterocycles differ from all carbon ring analogs in their physico-chemical characteristics due to the substitution of one or more carbon atoms with heteroatoms. Heterocycles are used in many different fields, such as veterinary, pharmaceutical, and agrochemical. These substances are also utilized in copolymers, corrosion inhibitors, antioxidants, and sanitizers. More than 85% of all physiologically active chemical compounds contain heterocycles, according to research. Pharmacological action is seen by all heterocycles, both natural and manufactured. Because of their diverse structures and adaptable characteristics, heterocyclic molecules are essential in medical chemistry. They are essential in the design and development of drugs because the addition of heteroatoms like nitrogen, oxygen, or sulfurs to their ring topologies increases their interaction with biological targets. Examples of heterocyclic compounds with unique features include pyridine, pyrrole, furan, and thiophene. Each of these compounds makes a unique contribution to the creation and manufacturing of pharmaceuticals.

Relevant conflicts of interest/financial disclosures: The authors declare that the research was conducted in the absence of any commercial or financial relationships that could be construed as a potential conflict of interest.

Compound	Name	Mol. Wt. (gm/mol)	2D Structure
1	7H-furo[3,2-g]-2H-chromen-7-one	186.16	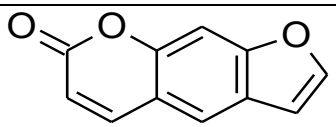
2	4-phenyl-2H-chromen-2-one	222.24	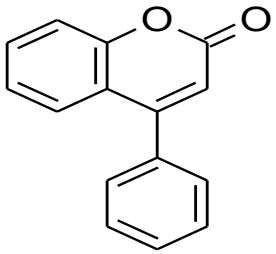
3	7-methoxy-8-(3-methylbut-2-enyl)-2H-chromen-2-one	244.28	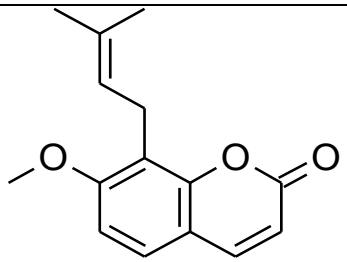
4	7-hydroxy-6-methoxy-2H-chromen-2-one	192.17	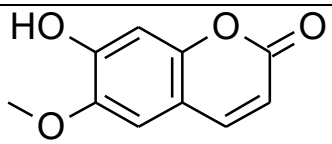
5	4-hydroxy-3-(1-phenylpropyl)-2H-chromen-2-one	280.3	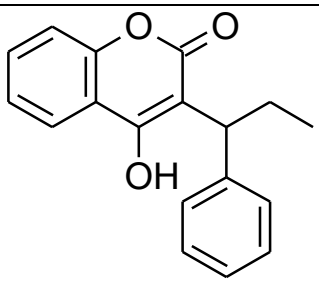
6	3-(2-oxo-2H-chromen-4-yl)-2H-chromen-2-one	290.3	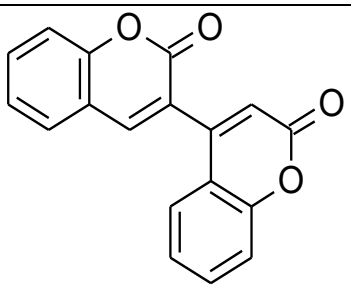
7	8-methoxy-4-methyl-2h-benzo[g]-2H-chromen-2-one	240.25	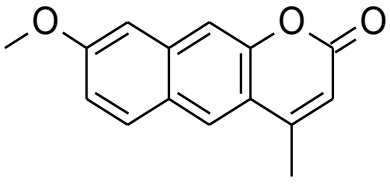

8	6,7-dihydroxy-4-methyl-2H-benzopyran-2-one	192.17	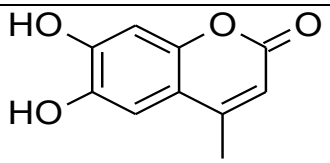
9	7-methoxy-2H-chromen-2-one	176.17	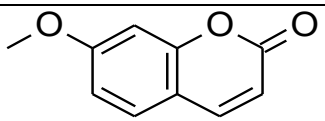
10	2,5,9-trimethylfuro[3,2-g]-2H-chromen-7-one	228.24	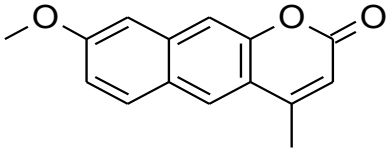
11	7-methoxychromen-2-one	176.17	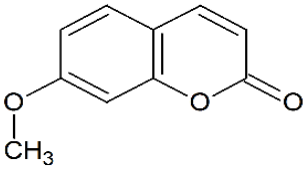
12	9-methoxy-7H-furo[3,2-g]chromen-7-one	216.19	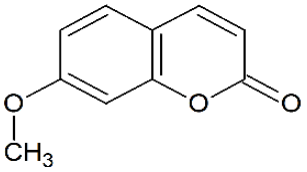
13	3,4-Dimethyl-7methoxychromen-2-one	228.24	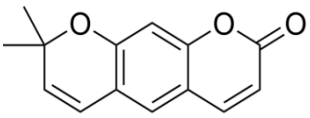
14	8,8-dimethyl-2H,8H-benzol[1,2-b:3,4-b]dipyran-2-one	228.24	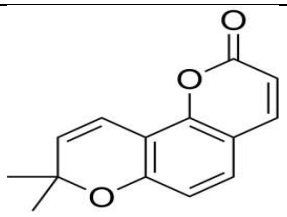
15	6-Hydroxy-5,7-dimethoxy coumarin	222.19	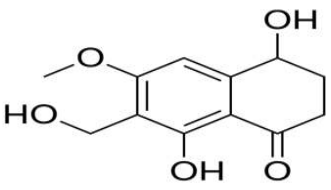

16	4-hydroxy-3-(3-oxo-1-phenylbuty l)-2H-chromen-2-one	308.33	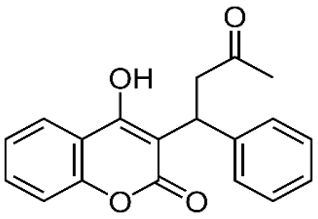
17	7-hydroxy-4-methylcoumarin	176.17	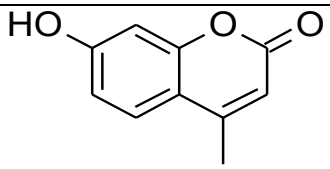
18	5-hydroxy-3,4-dimethyl-2H-chromen-2-one	216.19	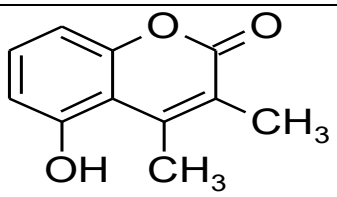
19	4-methoxy-7methyl-5H-furo[3,2-g]chromen-5-one	267.08	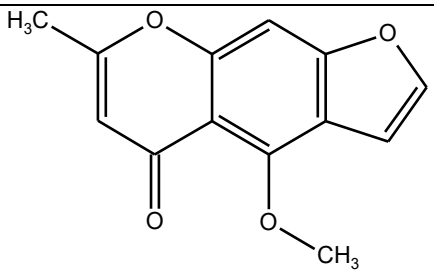
20	4,9-dimethoxy-7H-furo[3,2-g] chromen-7-one	186.16	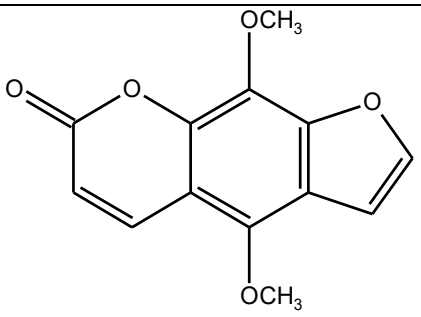
21	2-phenyl-4H-chromen-4-one	228.24	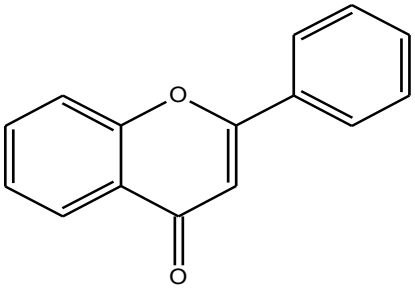

22	6-(dimethylamino)-8-methoxy-10 H-chromen[5,4,3]isoqunoline-10-one	206.19	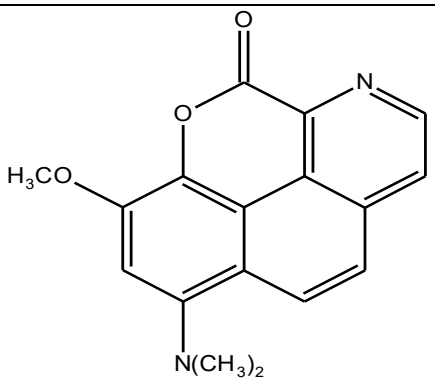
23	7-H-furo (3,2, -9) chromen-7-one	222.19	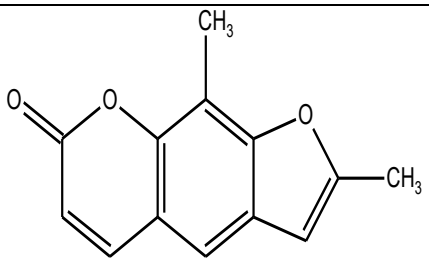
24	9-(isopentyloxy)-7H-furo[3,2-g] chromen-7-one	290.31	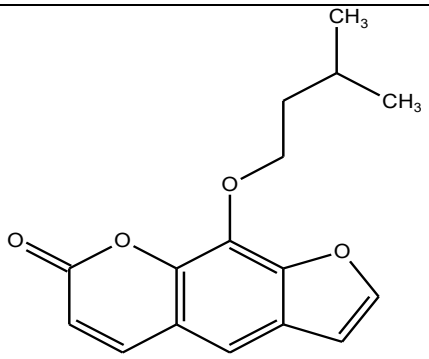
25	8-hydroxy-6,7-dimethoxychromen-2-one	222.19	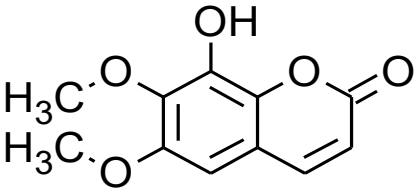

Table 1: Information about ligands

2. MATERIALS AND METHODS

Molecular Docking: To assess the possible binding behavior, all of the compounds undergo molecular docking using the Auto Dock 4.2 docking tool. For docking studies, the X-ray crystal structure of 1,3,4-oxadiazole (PDBID: 1OJA) was made available. ChemDraw Ultra 7.0 was first used to sketch the 2D structures of the ligands. Chem3D Ultra 7.0 was then used to transform these structures into three-dimensional arrangements. The PyMol program was used to save each structure in an a.pdb file. In order to utilize the structures with Auto Dock Vina 4.2, they were saved as PDBQT files. Docking simulations using AutoDock Vina produced nine distinct ligand-receptor conformations. The Discovery Studio Visualizer was used to analyze the final conformations.

Target Selection – The protein (target) related to the disease is selected. Target selection is the first step in molecular docking studies, where a suitable biological target protein related to the disease is chosen. The target is selected based on its role in disease progression and the availability of its 3D crystal structure. A well-characterized target with a known

active site helps in accurately predicting ligand–protein interactions.

Target Preparation – The protein structure is cleaned by removing water molecules, adding hydrogens, and optimizing it. Before docking, the protein structure is optimized by adding hydrogen atoms, removing water molecules, and correcting atomic clashes. The 3D crystal structure of protein (PDB ID: 1OJA) was obtained from the Protein Data Bank (RCSB).

Ligand Selection – Small molecules (e.g., coumarin derivatives) are chosen for docking. Ligand selection involves choosing small molecules or compounds that are expected to interact with the selected target protein. The ligands are selected based on their biological activity, chemical structure, and drug-like properties. These molecules are then prepared and used in docking studies to evaluate their binding affinity with the target.

Ligand Preparation – Ligands are energy minimized and optimized for proper geometry. Mol file formats were used as input for drug structures in computational studies. Therefore, the canonical SMILES of each drug were manually obtained from the PubChem database to generate the corresponding mol files. PubChem provides detailed information on drugs, including pharmacological data, clinical trial status, molecular weight, molecular formula, and both 2D and 3D structures.

Docking – Prepared ligands are placed into the active site of the target protein to predict binding. Docking is a computational technique used to predict how a ligand binds to the active site of a target protein. It helps in understanding the binding mode, binding affinity, and interactions between the ligand and protein. Docking results are analyzed to identify the most stable and effective ligand–protein complexes.

Evaluating Docking Results – Docking scores, binding energies, and interactions (H-bonds, hydrophobic, π–π) are analyzed to identify best hit compounds.

Pharmacokinetic Drug Likeliness: The ADMET properties of substances are linked to pharmacokinetic processes in the human body. Recently, computer-based drug development has shown increased interest in ADMET prediction by computational techniques studies. ADMET analyses are carried out to determine pharmacological structure from the standpoint of drug discovery. The SwissADME module of the SIB web server, accessible at https://www.sib.swiss, was used to examine the synthesized compounds for pharmacokinetic features, such as drug similarity, partition coefficient, solubility, and several other metrics. Each of the substances has substantial absorption in the gastrointestinal system. Every substance showed the ability to pass through the blood-brain barrier (BBB).

TPSA, drug likeness, and pharmacokinetic properties: The total number of hydrogen bonds, comprising both donors and accepters are significant indicators of this characteristic. Log P for the partition coefficient and Molecular weight, and hydrogen bonds in the molecule are a few examples of these descriptors. Rule of Five by Lipinski illustrates a substance's oral bioavailability by indicating the degree of permeability or absorption in lipid bilayers found within the human body. An additional characteristic that can be used to assess a drug's permeability is its ability to form hydrogen bonds. When a molecule has more than ten Hydrogen bond acceptors, five Hydrogen bond donors, the likelihood of poor penetration or absorption increases. (TPSA) has been used to describe drug consumption, including abdomen consumption, bioavailability, CaCO2 permeability, blood brain barrier permeability.

Boiled EGG PLOT analysis: ADMET, toxicity, efficacy, limited bioavailability, and pharmacokinetics are further repercussions of drug development issues. Investigations show that a high BBB crossover is possible when synthesized derivative inclining occurs inside the yellow loop. Compounds in the white "egg white" area are predicted to have high GI absorption, while those in the yellow "yolk" area are likely to cross the BBB.

Physicochemical Properties					Drug Likeness				
Compound	**Mol.wt .(gm)**	**H-acceptor**	**H-donor**	**Log *p***	**Total Polar Surface Area (TPSA)**	**Lipinski Violations**	**Ghose Violations**	**Veber Violations**	**Bioavaiability Score**
7H-furo[3,2-g]-2H-chromen-7-one	186.16	3	0	2.01	43.35	0	0	0	0.55
4-phenyl-2H-chromen-2-one	222.24	2	0	2.48	30.21	0	0	0	0.55
7-methoxy-8-(3-methylbut-2-enyl)-2H-chromen-2-one	244.28	3	0	2.93	39.44	0	0	0	0.55
7-hydroxy-6-methoxy-2H-chromen-2-one	192.17	4	1	1.95	59.67	0	0	0	0.55
4-hydroxy-3-(1-phenylpropyl)-2H-chromen-2-one	280.3	3	1	2.77	50.44	0	0	0	0.55
3-(2-oxo-2H-chromen-4-yl)-2H-chromen-2-one	290.3	4	0	2.54	60.42	0	0	0	0.55
8-methoxy-4-methyl-2H-benzo[g]-2H-chromen-2-one	240.25	3	0	2.69	39.44	0	0	0	0.55
6,7-dihydroxy-4-methyl-2H-benzopyran-2-one	192.17	4	2	1.52	70.67	0	0	0	0.55
7-methoxy-2H-chromen-2-one	176.17	3	0	2.06	39.44	0	0	0	0.55
2,5,9-trimethylfuro[3,2-g]-2H-chromen-7-one	228.24	3	0	2.72	43.35	0	0	0	0.55

7-methoxychromen-2-one	176.17	3	0	2.06	39.44	0	0	0	0.55
9-methoxy-7H-furo[3,2-g]chromen-7-one	216.19	5	0	2.09	30.21	0	0	0	0.55
3,4-Dimethyl-7 methoxychromen-2-one	228.24	5	0	2.62	39.44	0	0	0	0.55
8,8-dimethyl-2H,8H-benzol[1,2b:3,4b] dipyran-2-one	228.24	3	0	2.66	39.44	0	0	0	0.55
6-Hydroxy-5,7-dimethoxycoumarin	222.19	3	1	0.00	48.67	0	0	0	0.55
4-hydroxy-3-(3-oxo-1-phenylbutyl)-2H-chromen-2-one	308.33	5	0	2.41	67.51	0	0	0	0.55
7-hydroxy-4-methylcoumarin	176.17	3	1	1.81	50.44	0	0	0	0.55
5-hydroxy-3,4-dimethyl-2H-chromen-2-one	216.19	5	0	3.73	76.74	0	0	0	0.55
4-methoxy-7methyl -5H-furo[3,2-g] Chromen-5-one	267.08	4	0	3.88	52.58	0	0	0	0.55
4,9-dimethoxy-7H-furo[3,2-g]chromen-7-one	186.16	4	0	2.86	52.58	0	0	0	0.55
2-phenyl-4H-chromen-4-one	228.24	3	0	2.54	43.35	0	0	0	0.55
6-(dimethylamino)-8-methoxy-10H-chromen[5,4,3] isoqunoline-10-one	206.19	5	0	3.04	55.57	0	0	0	0.55

7-H-furo (3,2, -9) chromen-7-one	222.19	3	1	2.12	50.44	0	0	0	0.55
9-(isopentyloxy)-7H-furo[3,2-g]chromen-7-one	290.31	3	0	1.80	39.44	0	0	0	0.55
8-hydroxy-6,7-dimethoxychromen-2-one	222.19	5	1	1.99	68.90	0	0	0	0.55

Table 2: Lipinski factors for drug similarity qualities of coumarin derivatives, absorption distribution, and metabolism elimination characteristics.

Compound	GI Absorption	P-gp	CYP1A2 Inhibitor	CYP2C19 Inhibitor	CYP2D6 Inhibitor
7H-furo[3,2-g]-2H-chromen-7-one	High	No	Yes	No	No
4-phenyl-2H-chromen-2-one	High	No	Yes	Yes	No
7-methoxy-8-(3-methylbut-2-enyl)-2H-chromen-2-one	High	No	Yes	Yes	No
7-hydroxy-6-methoxy-2H-chromen-2-one	High	No	Yes	No	No
4-hydroxy-3-(1-phenylpropyl)-2H-chromen-2-one	High	No	Yes	Yes	Yes
3-(2-oxo-2H-chromen-4-yl)-2H-chromen-2-one	High	No	Yes	Yes	No
8-methoxy-4-methyl-2H-benzo[g]-2H-chromen-2-one	High	No	Yes	Yes	No
6,7-dihydroxy-4-methyl-2H-benzopyran-2-one	High	No	Yes	No	No
7-methoxy-2H-chromen-2-one	High	No	Yes	No	No
2,5,9-trimethylfuro[3,2-g]-2H-chromen-7-one	High	No	Yes	Yes	No
7-methoxychromen-2-one	High	No	Yes	No	No
9-methoxy-7H-furo[3,2-g]chromen-7-one	High	No	Yes	Yes	No

3,4-Dimethyl-7methoxychromen-2-one	High	No	Yes	Yes	No
8,8-dimethyl-2H,8H-benzol[1,2b:3,4b]dipyran-2-one	High	No	Yes	Yes	No
6-Hydroxy-5,7-dimethoxycoumarin	High	No	Yes	No	No
4-hydroxy-3-(3-oxo-1-phenylbutyl)-2H-chromen-2-one	High	No	Yes	Yes	No
7-hydroxy-4-methylcoumarin	High	No	Yes	No	No
5-hydroxy-3,4-dimethyl-2H-chromen-2-one	High	Yes	No	No	No
4-methoxy-7methyl-5H-furo[3,2-g]Chromen-5-one	High	No	Yes	Yes	No
4,9-dimethoxy-7H-furo[3,2-g]chromen-7-one	High	No	Yes	No	No
2-phenyl-4H-chromen-4-one	High	No	Yes	No	No
6-(dimethylamino)-8-methoxy-10H-chromen[5,4,3]isoqunoline-10-one	High	No	Yes	Yes	Yes
7-H-furo (3,2, -9) chromen-7-one	High	No	Yes	No	No
9-(isopentyloxy)-7H-furo[3,2-g]Chromen-7-one	High	No	Yes	No	No
8-hydroxy-6,7-dimethoxychromen-2-one	High	No	Yes	No	No

Table 3: Pharmacokinetic Prediction of coumarin derivatives using SWISS ADME.

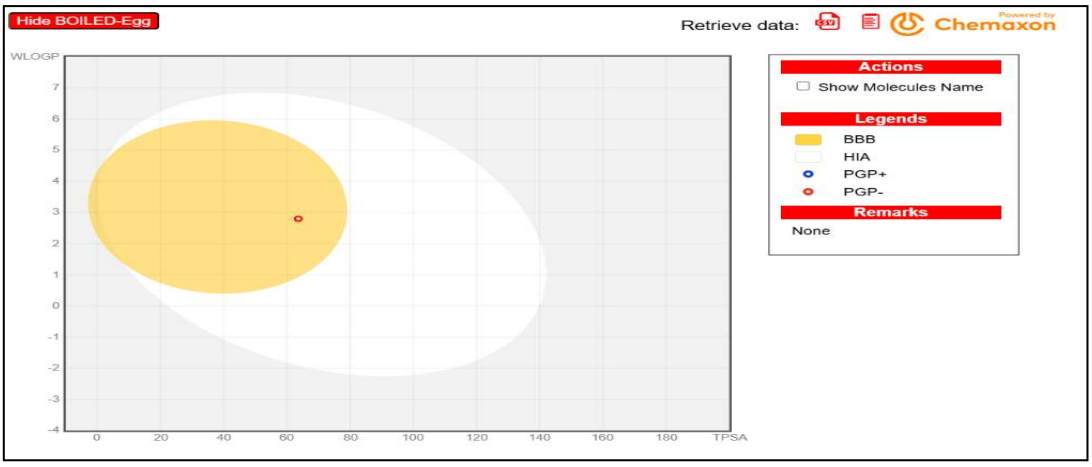

Figure 1: Boiled Egg Plot of most effective Virtual Screened .

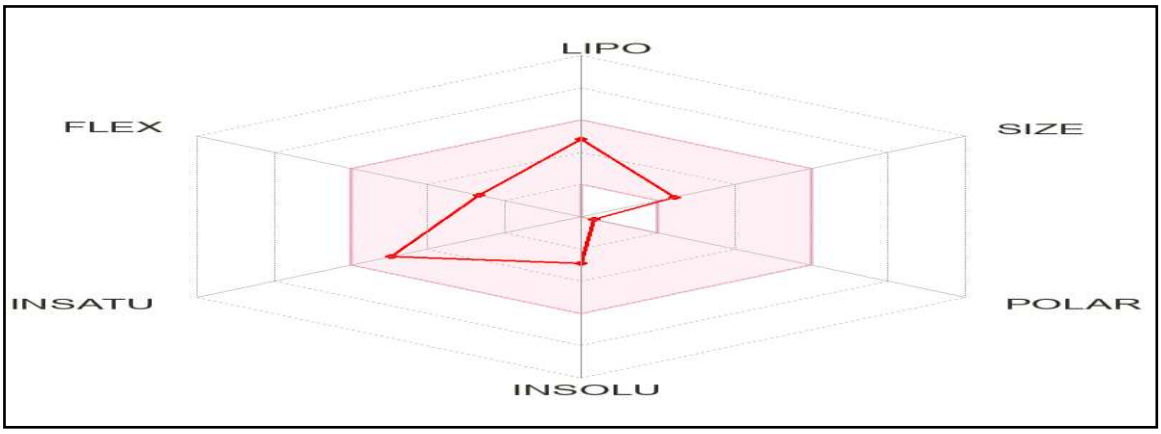

Figure 2: Selegiline bioavailability radar is displayed for the following compounds: LIPO (lipophilicity as XLOGP3), SIZE (size as molecular weight), POLAR (polarity as TPSA), INSOLU (insolubility in water by log S scale), INSATU (in saturation as per fraction of carbons in the sp3 hybridization), and FLEX (flexibility as per rotatable bond).

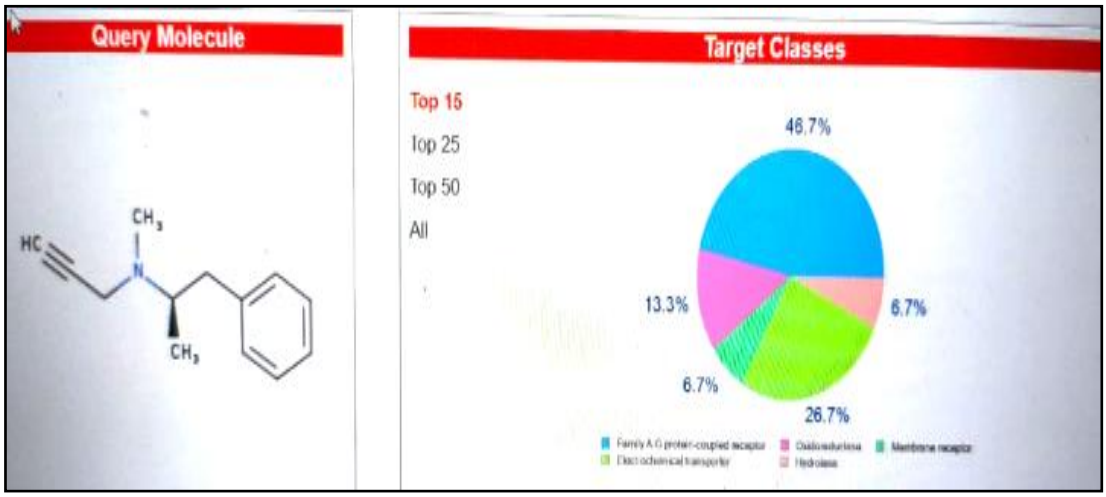

Target	Common name	Uniprot ID	ChEMBL ID	Target Class	Probability*	Known actives (3D/2D)
Alpha-2a adrenergic receptor	ADRA2A	P08913	CHEMBL1867	Family A G protein-coupled receptor		25 / 5
Alpha-2b adrenergic receptor	ADRA2B	P18089	CHEMBL1942	Family A G protein-coupled receptor		25 / 9
Monoamine oxidase A	MAOA	P21397	CHEMBL1951	Oxidoreductase		49 / 73
Monoamine oxidase B	MAOB	P27338	CHEMBL2039	Oxidoreductase		44 / 79
Sigma opioid receptor	SIGMAR1	Q99720	CHEMBL287	Membrane receptor		260 / 299
Synaptic vesicular amine transporter *(by homology)*	SLC18A2	Q05940	CHEMBL1893	Electrochemical transporter		18 / 67
Dopamine transporter	SLC6A3	Q01959	CHEMBL238	Electrochemical transporter		535 / 371
Dopamine D2 receptor *(by homology)*	DRD2	P14416	CHEMBL217	Family A G protein-coupled receptor		231 / 203
Serotonin transporter *(by homology)*	SLC6A4	P31645	CHEMBL228	Electrochemical transporter		653 / 370
Trace amine-associated receptor 1 *(by homology)*	TAAR1	Q96RJ0	CHEMBL5857	Family A G protein-coupled receptor		4 / 9
Dopamine D3 receptor *(by homology)*	DRD3	P35462	CHEMBL234	Family A G protein-coupled receptor		121 / 95
Serotonin 2a (5-HT2a) receptor	HTR2A	P28223	CHEMBL224	Family A G protein-coupled receptor		272 / 61

Figure 3: An example of the Swiss Target Prediction Report of Compound Selegiline.

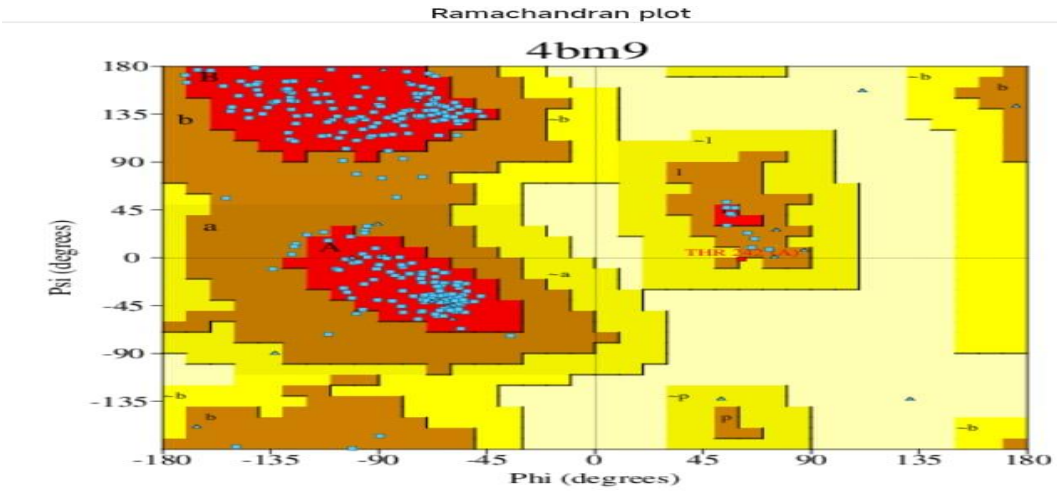

Figure 4: Ramachandran Plot of Protein Molecule (4BM9)

PROCHECK statistics

1. Ramachandran Plot statistics

		No. of residues	%-tage
Most favoured regions	[A,B,L]	222	87.7%*
Additional allowed regions	[a,b,l,p]	30	11.9%
Generously allowed regions	[~a,~b,~l,~p]	1	0.4%
Disallowed regions	[XX]	0	0.0%
Non-glycine and non-proline residues		253	100.0%
End-residues (excl. Gly and Pro)		8	
Glycine residues		20	
Proline residues		20	
Total number of residues		301	

Figure 5: PROCHECK statistics of Protein Molecule (4BM9)

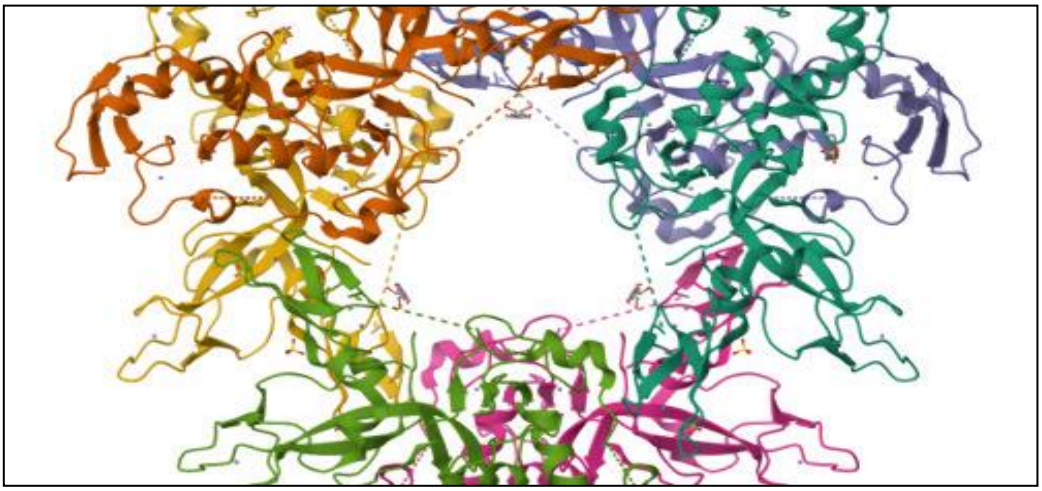

Figure 5: 3D Structure of 4BM9

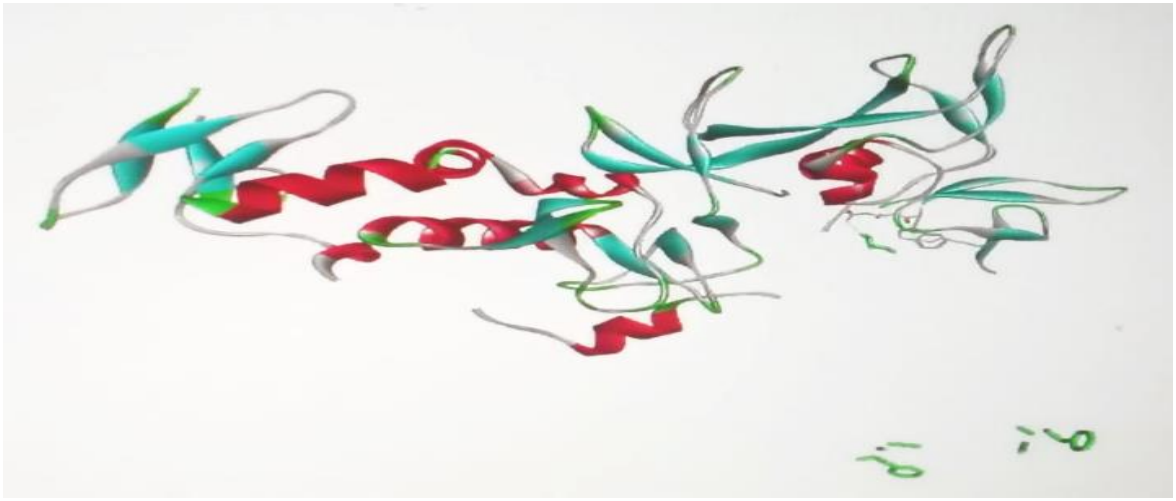

Figure 6: 3D interaction of protein (4BM9) with ligand

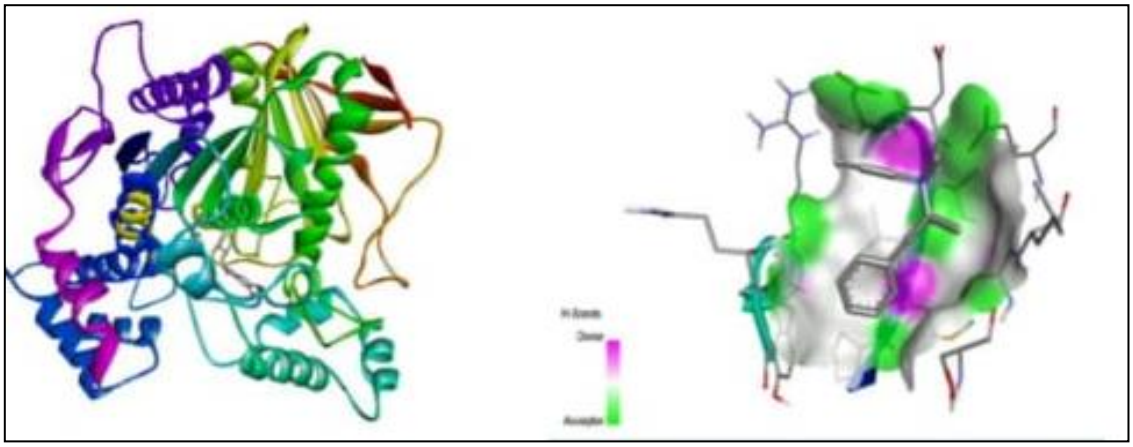

Figure 7: 3D visualization of standard Selegiline by using Discovery studio.

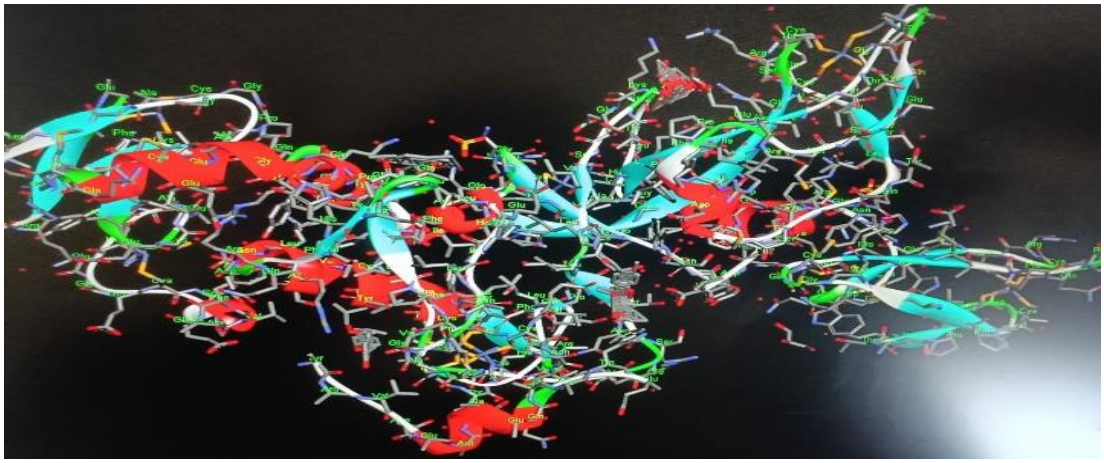

Figure 12: This image shows protein–ligand interaction visualization after molecular docking (amino-acid residues labeled around a bound ligand).

RESULT

Molecular Docking study was performed on Twenty five derivatives of Coumarin

Drug	Docking Score	Docking Image
7H-furo[3,2-g]-2H-chromen-7-one	-9.0	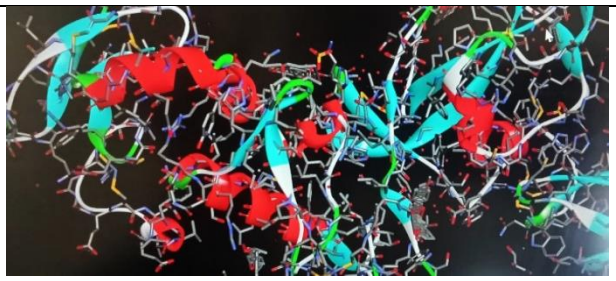
4-phenyl-2H-chromen-2-one	-8.9	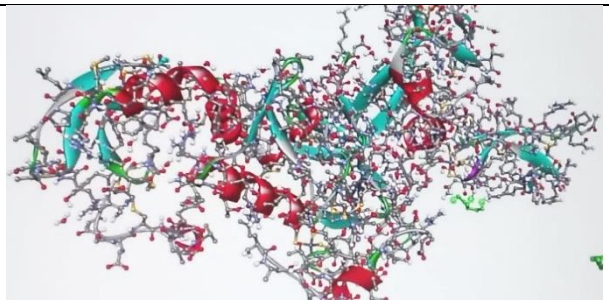
7-methoxy-8-(3-methylbut-2-enyl) -2H-chromen-2-one	-6.8	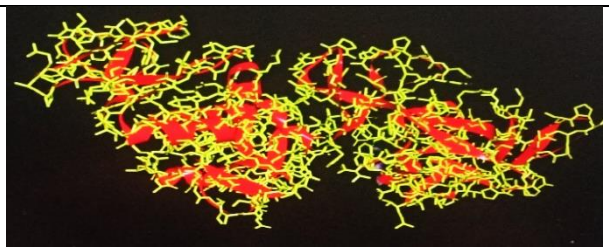
7-hydroxy-6-methoxy-2H-chromen-2 -one	-9.8	
4-hydroxy-3-(1-phenylpropyl)-2H- chromen-2-one	-8.9	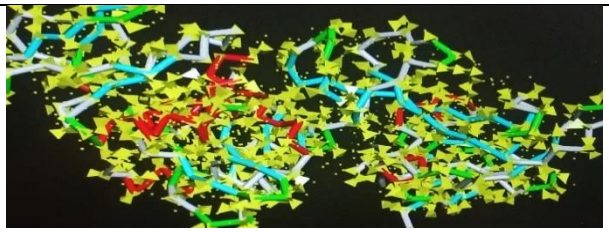
3-(2-oxo-2H-chromen-4-yl)-2H-chromen-2-one	-8.6	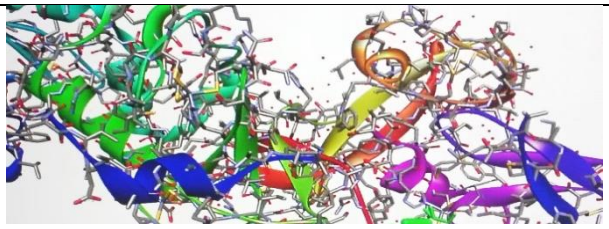

8-methoxy-4-methyl-2h-benzo[g]-2H -chromen-2-one	-7.3	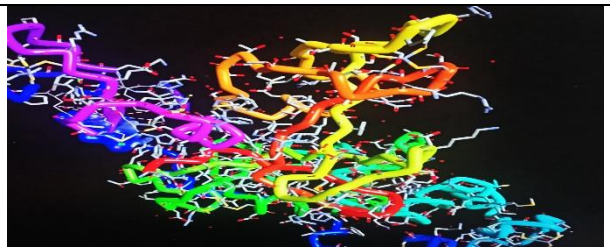
6,7-dihydroxy-4-methyl-2H- benzopyran-2-one	-7.0	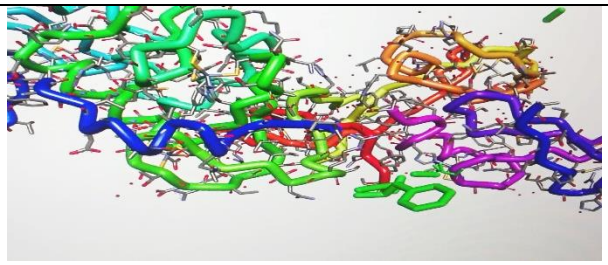
7-methoxy-2H-chromen-2-one	-8.7	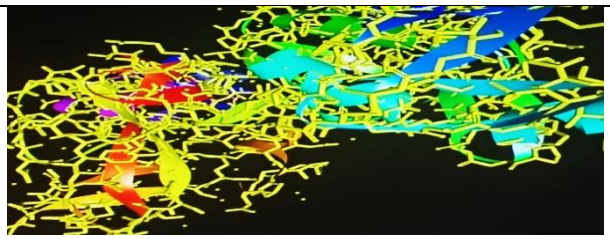
2,5,9-trimethylfuro[3,2-g]-2H- chromen-7-one	-8.9	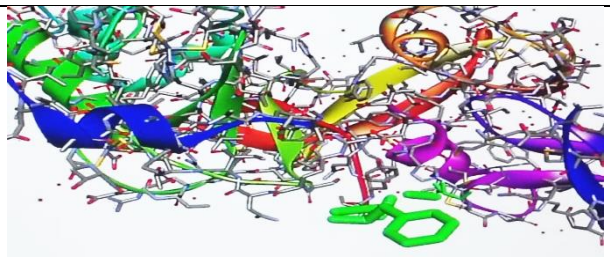
7-methoxychromen-2-one	-7.0	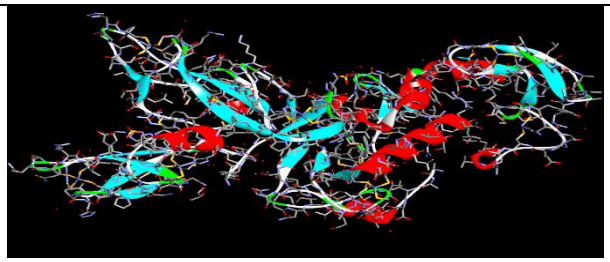
9-methoxy-7H-furo[3,2-g]chromen-7 -one	-7.9	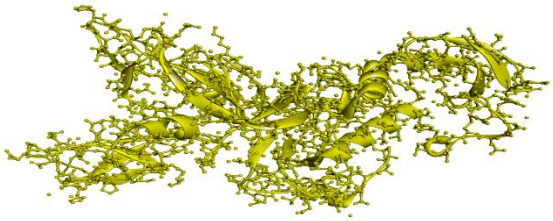

3,4-Dimethyl-7-methoxychromen-2-one	-8.6	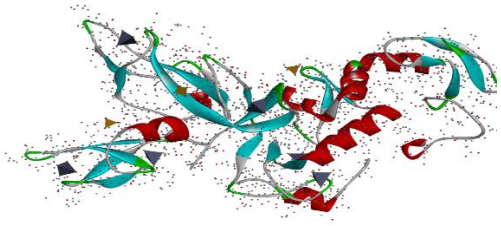
8,8-dimethyl-2H,8H-benzol[1,2-b:3,4-b]dipyran-2-one	-7.6	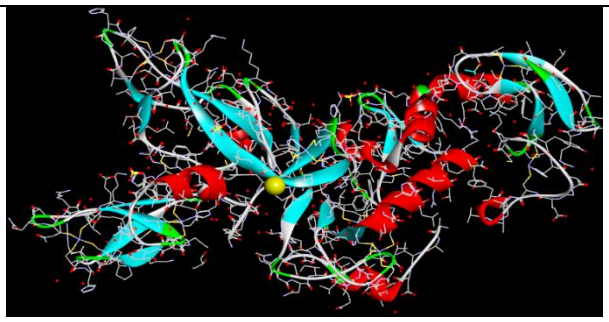
6-Hydroxy-5,7-dimethoxycoumarin	-8.7	
4-hydroxy-3-(3-oxo-1-phenylbutyl)-2H-chromen-2-one	-9.0	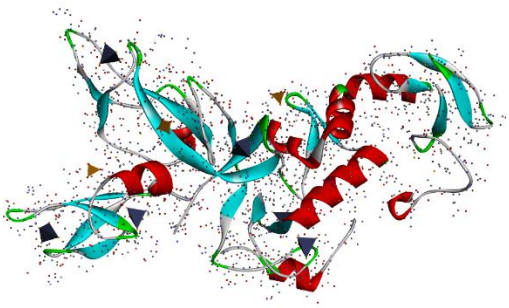
7-hydroxy-4-methylcoumarin	-7.2	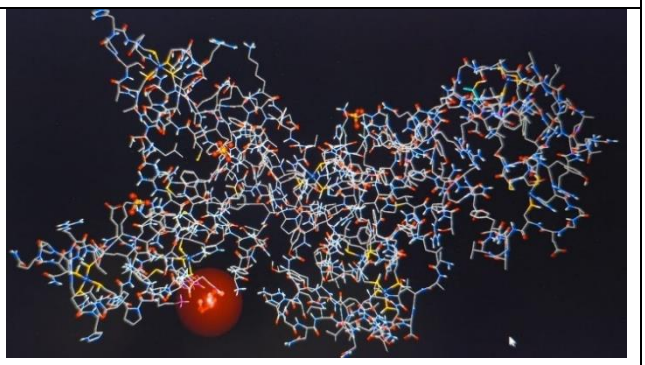

5-hydroxy-3,4-dimethyl-2H-chromen -2-one	-6.6	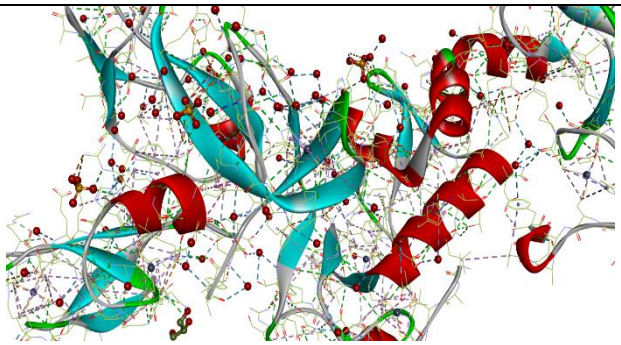
4-methoxy-7methyl-5H-furo[3,2-g] chromen-5-one	-7.5	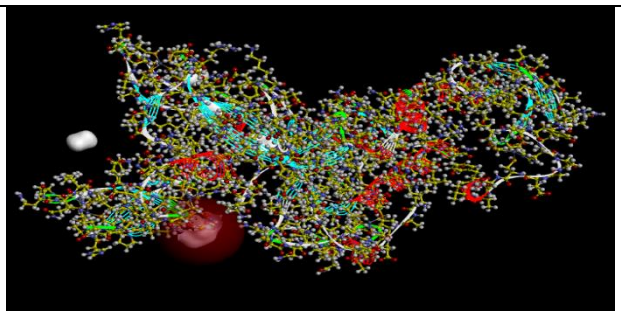
4,9-dimethoxy-7H-furo[3,2-g] chromen-7-one	-7.7	
2-phenyl-4H-chromen-4-one	-8.4	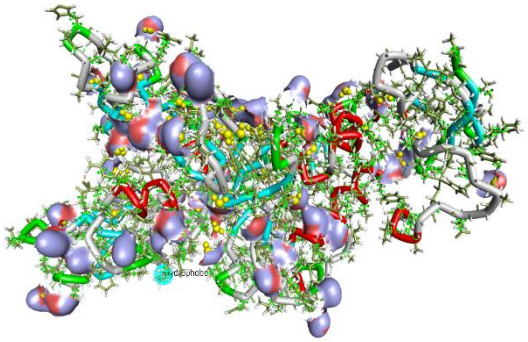
6-(dimethylamino)-8-methoxy-10H-chromen[5,4,3]isoqunoline-10-one	-9.9	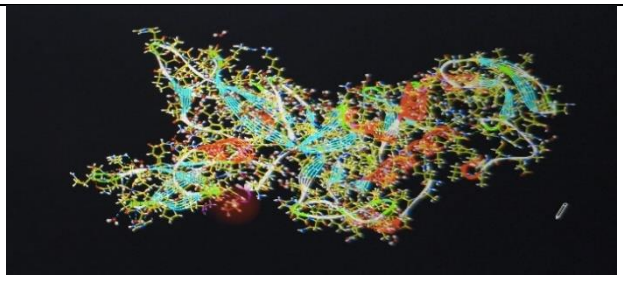

4-methoxyfuro[3,2-g]chromen-7-one	-7.5	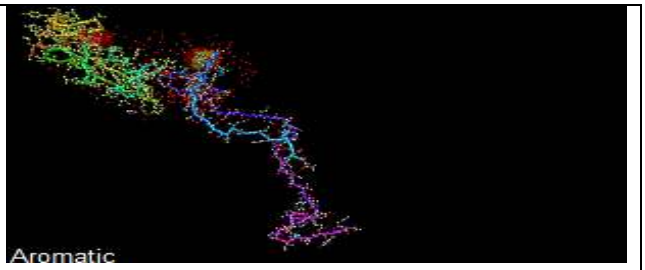
7-H-furo (3,2,9) chromen-7-one	-8.5	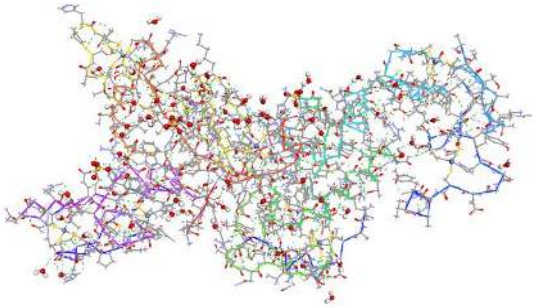
9-(isopentyloxy)-7H-furo[3,2-g] chromen-7-one	-8.0	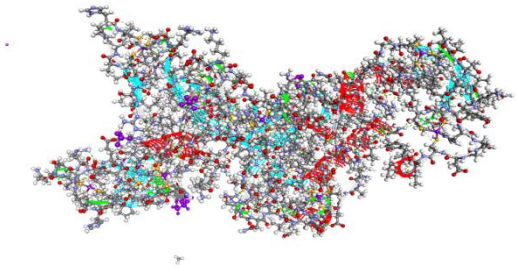
8-hydroxy-6,7-dimethoxychromen-2-one	-7.5	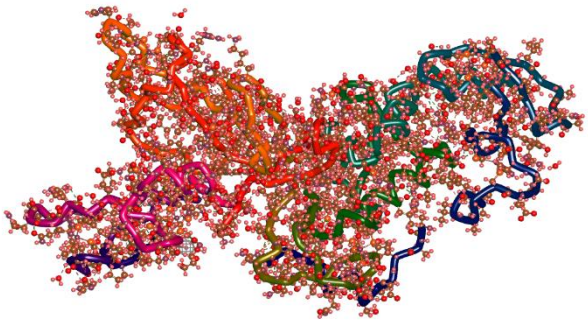

CONCLUSION

In the present study, twenty-five coumarin derivatives were evaluated using molecular docking and *in silico* ADMET analysis to assess their potential as drug candidates. Several compounds demonstrated favorable binding affinities toward the selected target protein, with **6-(dimethylamino)-8-methoxy-10H-chromen [5,4,3] isoquinoline-10-one** exhibiting the highest docking score among the tested derivatives. Drug-likeness and pharmacokinetic evaluation using SwissADME indicated that most compounds complied with Lipinski's Rule of Five, possessed high gastrointestinal absorption, and showed acceptable pharmacokinetic properties with minimal predicted toxicity. These findings suggest that coumarin derivatives represent promising lead molecules for further drug discovery. However, the present results are based solely on computational analysis; therefore, **in vitro**, **in vivo**, and further pharmacological investigations are required to validate their biological activity, safety, and therapeutic potential.

REFERENCES

1. Shetty CR, Bhat KI, Kumar A, Kumar P, Krishnamurthy PT, Merugumolu VK. Synthesis,

in-silico studies and evaluation of anticancer activity of some novel benzothiazole substituted 4-thiazolidinones. Indian J Pharmaceut Educ Res. 2020 Oct 1; 54:1121-32.

2. Anaridha S, PK MI, MEERAN S, Shabeer TK. Computational analysis using ADMET profiling, DFT calculations and molecular docking of two anti-cancer drugs. Turkish Computational and Theoretical Chemistry.;7(1):37-50.
3. Purwanto BT, Hardjono S, Widiandani T, Nasyanka AL, Siswanto I. In Silico Study and ADMET prediction of N-(4-fluorophenylcarbamothioyl) Benzamide Derivatives as Cytotoxic Agents. Journal of Hunan University Natural Sciences. 2021 Mar 26;48(2).
4. Sharma V, Sharma PC, Kumar V. In silico molecular docking analysis of natural pyridoacridines as anticancer agents. Advances in Chemistry. 2016 Nov;(5409387):1-9.
5. Al-Blewi F, Shaikh SA, Naqvi A, Aljohani F, Aouad MR, Ihmaid S, Rezki N. Design and synthesis of novel imidazole derivatives possessing triazole pharmacophore with potent anticancer activity, and in silico ADMET with GSK-3β molecular docking investigations. International journal of molecular sciences. 2021 Jan 25;22(3):1162.
6. De Oliveira CS, Lira BF, Barbosa-Filho JM, Lorenzo JG, de Athayde-Filho PF. Synthetic approaches and pharmacological activity of 1, 3, 4-oxadiazoles: a review of the literature from 2000–2012. Molecules. 2012 Aug 27;17(9):10192-231.
7. Hussain A, Verma CK. Molecular docking and in silico ADMET study reveals 3-(5-{[4-(aminomethyl) piperidin-1-yl] methyl}-1h-indol-2-yl)-1h-indazole-6-carbonitrile as a potential inhibitor of cancer Osaka thyroid kinase. Biomed Res. 2017 Jan 1;28(13):5805- 15.
8. Yalcin S. Molecular Docking, Drug Likeness, and ADMET Analyses of Passiflora compounds as P-glycoprotein (P-gp) inhibitor for the treatment of cancer. Current Pharmacology Reports. 2020 Dec;6:429-40.
9. SundariIlangovan S, Subash R, Janani N,Ishwarya P. Predicting ADMET Properties for Commercially Available Anticancer Drugs. International Journal of Innovative Technology and Exploring Engineering Journal of Technology VOLUME 12 ISSUE 5, 2024 ISSN: 10123407 PAGE NO:275
10. Refsgaard HH, Jensen BF, Brockhoff PB, Padkjær SB, Guldbrandt M, Christensen MS. In silico prediction of membrane permeability from calculated molecular parameters. Journal of medicinal chemistry. 2005 Feb 10;48(3):805-11.
11. Muegge I. Selection criteria for drug-like compounds. Medicinal research reviews. 2003 May;23(3):302-21.
12. Merdekawati F. In silico study of pyrazolylaminoquinazoline toxicity by lazar, protox, and admet predictor. Journal of Applied Pharmaceutical Science. 2018 Sep 30;8(9):119-29.
13. Veber DF, Johnson SR, Cheng HY, Smith BR, Ward KW, Kopple KD. Molecular properties that influence the oral bioavailability of drug candidates. Journal of medicinal chemistry. 2002 Jun 6;45(12):2615-23.
14. Bojarska J, Remko M, Breza M, Madura ID, Kaczmarek K, Zabrocki J, Wolf WM. A supramolecular approach to structure-based design with a focus on synthons hierarchy in ornithine-derived ligands: Review, synthesis, experimental and in silico studies. Molecules. 2020 Mar 3;25(5):1135.
15. Daina A, Zoete V. A boiled-egg to predict gastrointestinal absorption and brain penetration of small molecules. ChemMed. 2016 Jun 6;11(11):1117-21.
16. 16. Daina A, Michielin O, Zoete V. SwissADME: a free web tool to evaluate pharmacokinetics, drug-likeness and medicinal chemistry friendliness of small molecules. Scientific reports. 2017 Mar 3;7(1):42717.
17. Amin ML. P-glycoprotein inhibition for optimal drug delivery. Drug target insights. 2013 Jan;7:DTI-S12519.
18. Jadhav SA, Sen DB, Sen AK, Shah AP. In silico Pharmacokinetics and Docking Analysis of Active Biomolecules from 5-Amino-Salicylic Acid against Cyclin Dependent Kinase II. NeuroQuantology. 2022;20(9):364.
19. Ripphausen P, Stumpfe D, Bajorath J. Analysis of structure-based virtual screening studies and characterization of identified active compounds.

Future Medicinal Chemistry. 2012 Apr;4(5):603-13.

20. Mirza MU, Ghori NU, Ikram N, Adil AR, Manzoor S. Pharmacoinformatics approach for investigation of alternative potential hepatitis C virus nonstructural protein 5B inhibitors. Drug design, development and therapy. 2015 Mar 27:1825-41.
21. Nisha CM, Kumar A, Nair P, Gupta N, Silakari C, Tripathi T, Kumar A. Molecular docking and in silico ADMET study reveals acylguanidine 7a as a potential inhibitor of β-secretase. Advances in bioinformatics. 2016.
22. Ceci C, Atzori MG, Lacal PM, Graziani G. Role of VEGFs/VEGFR-1 signaling and its inhibition in modulating tumor invasion: Experimental evidence in different metastatic cancer models. International journal of molecular sciences. 2020 Feb 18;21(4):1388.
23. Barber RD. Software to visualize proteins and perform structural alignments. Current Protocols. 2021 Nov;1(11):e292.
24. Vina A. Improving the speed and accuracy of docking with a new scoring function, efficient optimization, and multithreading Trott, Oleg; Olson, Arthur J. J. Comput. Chem. 2010;31(2):455-61.

HOW TO CITE: Vivekanand Ekanath Teli*, Rutuja Ashok Vyawahare, Bhumika Bhairu Mohite, Dipali Vijay Patil, In Silico Molecular Docking And ADMET Evaluation Of Coumarin Derivatives As Potential Therapeutic Lead Compounds, Int. J. Sci. R. Tech., 2026, 3 (7), 97-116. https://doi.org/10.5281/zenodo.21237576